Millimeter-Wave Attenuation and Delay Rates Due to Fog/Cloud Conditions

HANS J. LIEBE, FELLOW, IEEE, TAKESHI MANABE, MEMBER, IEEE, AND GEORGE A. HUFFORD, MEMBER, IEEE

Abstract—**Propagation properties of suspended water and ice particles which make up atmospheric haze, fog, or clouds were examined for microwave and millimeter-wave frequencies. Rates of attenuation α (dB/km) and delay τ (ps/km) are derived from a complex refractivity based on the Rayleigh absorption approximation of Mie's scattering theory. Key variables are particle mass content and permittivity which depends on frequency and temperature, both for liquid and ice states. Water droplet attenuation can be estimated within a restricted (10 ± 10°C) temperature range using a simple two-coefficient approximation. Experimental data on signal loss and phase delay caused by fog at four frequencies (50, 82, 141, and 246 GHz) over a 0.81-km line-of-sight path were found to be consistent with the described model.**

I. Introduction

MILLIMETER-WAVE applications in communications, active and passive sensing, radio astronomy, etc. are progressing steadily. Among the well-documented attributes of millimeter waves is their decisive advantage over infrared and optical waves when obscuration effects due to atmospheric aerosols impose intolerable restrictions on system performance. For assessing the potential benefits of operating in the 30 to >300 GHz range, system designers have to rely on realistic atmospheric propagation models capable of predicting attenuation and delay by suspended water droplets (SWD) and ice crystals (SIC) present under haze, fog, or cloud conditions.

Propagation effects of the air mass which hosts SWD and SIC aerosols can be evaluated with a millimeter-wave propagation model (MPM) by specifying four input parameters: frequency f (GHz), total pressure P (kPa), temperature T (°C), and relative humidity RH (percent) [1], [2]. Basic, strongly frequency-dependent limitations are imposed by molecular oxygen and water vapor. The model considers 48 O_2 plus 30 H_2O absorption lines centered below 1000 GHz complemented by continuum spectra. In clear air, experimental transmission (signal loss and delay) and emission data were found to be consistent with MPM predictions at selected frequencies between 28 and 430 GHz [2]–[4].

Water and ice particles in fogs or clouds influence millimeter waves by means of their concentration w (g/m^3). Generally, the supporting air mass has to reach a slightly supersaturated (100–101 percent RH) state to produce significant values of w ($>10^{-3}$ g/m^3). To calculate propagation effects, the Rayleigh absorption approximation can be applied to replace the much more complicated Mie scattering theory [5]. That way, the microstructure of the particular SWD or SIC aerosol is ignored. In the past only the loss part of the Rayleigh formulation has been applied [6]–[8]. Knowing the correct correspondence at a given frequency permits results from transmission measurements to be interpreted as a measure of path-averaged particle content [9]. Above 100 GHz, a review has shown that predicted SWD attenuation exceeds established values when up-to-date results for the permittivity of water are applied [10]. This paper will elaborate on

- a model that predicts for suspended particles the frequency (f) and temperature (T) variability of attenuation and delay from revised formulations for complex permittivities of both liquid water [11] and ice [12] (Section II);
- a simple expression for estimating SWD attenuation as an alternative to one discussed in [13] (Section III); and
- an analysis of experimental data for signal loss and phase delay obtained at four frequencies between 50 and 246 GHz during a fog event over a 0.81-km line-of-sight path with a system described in [14] (Section IV).

II. Propagation Model for Suspended Particles

A. Propagation and Rayleigh Terms

The interaction between radio waves and atmospherically suspended particles is described by a complex refractivity in parts per million (10^{-6}) [1]

$$N = N_0 + N'(f) - jN''(f) \quad \text{ppm}, \tag{1}$$

where $j = \sqrt{-1}$, N_0 is independent of frequency, $N'(f)$ and $N''(f)$ represent refractivity and loss spectra, respectively. Refractivity (1) is fundamental to practical propagation terms such as power attenuation

$$\alpha = 0.1820\, fN''(f) \quad \text{dB/km}, \tag{2}$$

phase change

$$\beta = 1.2008\, f[N_0 + N'(f)] \quad \text{deg/km}, \tag{3}$$

or propagation delay

$$\tau = 3.3356\, [N_0 + N'(f)] \quad \text{ps/km}, \tag{4}$$

Manuscript received June 30, 1988, revised January 3, 1989. This work was supported in part by the Naval Ocean Systems Center (Ref: RA35 G80).

H. J. Liebe and G. A. Hufford are with the National Telecommunications and Information Administration, Institute for Telecommunication Sciences, Boulder, CO 80303-3328.

T. Manabe was with the National Telecommunications and Information Administration, Institute for Telecommunication Sciences, on leave from the Radio Research Laboratory, Ministry of Posts and Telecommunications, Koganei, Tokyo 184. He is now with ATR Optical and Radiocommunications Research Laboratories, Seika-cho, Soraku-gun, Kyoto 619-02, Japan.

IEEE Log Number 8932932.

where f is frequency in GHz (throughout this paper). The formulas and constants here come from the plane wave propagation factor $\exp[-2\pi jfL(1+N10^{-6})/c]$ and reductions to decibel, degree, or picosecond, where L is the length of the path and c is the speed of light in vacuum.

A refractivity model for SWD and SIC media derives from the Rayleigh absorption approximation [5],

$$N = w(3/2m_{w,i})(\epsilon - 1)/(\epsilon + 2) \quad \text{ppm}, \tag{5}$$

of Mie's forward scattering function, which provides both amplitude and phase information independent of the particle-size distribution. Mass content per unit of air volume is given by w in g/m^3; the specific weights are $m_w = 1.000$ for water and $m_i = 0.916$ g/cm^3 for ice (the mixture of units in w/m provides the unit ppm); and the complex permittivity of liquid water is $\epsilon = \epsilon'(f) - j\epsilon''(f)$ (or ϵ_i for ice). Equation (5) was rationalized to describe for the SWD medium nondispersive refractivity (N_0) and spectra of refractivity (N') and loss (N''):

$$N_0 = w(3/2)[1 - 3/(\epsilon_0 + 2)], \tag{6a}$$

$$N'(f) = w(9/2)[1/(\epsilon_0 + 2) - y/\epsilon''(y^2 + 1)], \tag{6b}$$

$$N''(f) = w(9/2)[\epsilon''(y^2 + 1)]^{-1}, \tag{6c}$$

with $y = (\epsilon' + 2)/\epsilon''$.

Permittivity of liquid water for $f = 0$ to 1000 GHz is computed with a new double-Debye formulation [11],

$$\epsilon = (\epsilon_0 - \epsilon_1)[1 + (f/f_P)] + (\epsilon_1 - \epsilon_2)/[1 + j(f/f_S)] + \epsilon_2. \tag{7}$$

Real and imaginary parts of (7) are

$$\epsilon'(f) = (\epsilon_0 - \epsilon_1)/[1 + (f/f_P)^2] + (\epsilon_1 - \epsilon_2)/[1 + (f/f_S)^2] + \epsilon_2 \tag{8a}$$

and

$$\epsilon''(f) = (\epsilon_0 - \epsilon_1)(f/f_P)/[1 + (f/f_P)^2] + (\epsilon_1 - \epsilon_2)(f/f_S)/[1 + (f/f_S)^2]. \tag{8b}$$

Three permittivity constants,

$$\epsilon_0(T) = 77.66 + 103.3(\theta - 1),$$

$$\epsilon_1 = 5.48 \quad \text{and} \quad \epsilon_2 = 3.51; \tag{8c}$$

in addition to principal and secondary relaxation frequencies,

$$f_P(T) = 20.09 - 142.4(\theta - 1) + 294(\theta - 1)^2 \quad \text{GHz},$$

and

$$f_S(T) = 590 - 1500(\theta - 1) \quad \text{GHz}, \tag{8d}$$

enter into the ϵ model. The relative inverse temperature variable, $\theta = 300/[T(°\text{C}) + 273.15]$, was adopted from the MPM program [1].

In summary, (2)–(8) represent the propagation model for suspended water droplets. Dielectric properties of bulk water are converted by means of (6) into refractivity spectra of the SWD medium.

Permittivity of ice was reevaluated by one of us (G.A.H.) resulting in the following real and imaginary parts [12]:

$$\epsilon_i' = 3.15 \tag{9a}$$

and

$$\epsilon_i''(f) = A_i/f + B_i f \tag{9b}$$

where

$$A_i = [50.4 + 62(\theta - 1)]10^{-4} \exp[-22.1(\theta - 1)]$$

and

$$B_i = (0.633/\theta - 0.131)10^{-4} + [7.36 \cdot 10^{-4}\,\theta/(\theta - 0.9927)]^2$$

(e.g., at $T = -10°\text{C}$ or $\theta = 1.140$: $\epsilon_i'' \approx 0.00035$, 0.001, 0.01, 0.1 for $f = 1$, 10, 100, 1000 GHz, respectively). Equation (9) fits experimental ϵ_i data from ≈ 1 MHz to 1 THz for $T \approx -40°$ to 0°C. Inserting (9) into (5), (2), and (3) provides estimates of the very low loss and delay effects by suspended ice crystals.

Propagation effects by SIC are of negligible consequence (see Section III) since ice clouds occur foremost as cirrus at high altitudes (>8 km) with little mass content ($w < 0.001$ g/m^3). Ice crystals appear in the shape of needles or plates that cause depolarization effects. The focus of all following discussion is on the liquid droplet state.

B. SWD Composition

Haze, fog, and nonprecipitating clouds are assumed to be composed of spherical water droplets with radii small enough ($r \leq 50$ μm) to keep them suspended in air by microturbulence. The total number of drops per unit volume represents a liquid water content,

$$w = (4\pi/3) \int n(r) r^3 \, dr \quad \text{g/m}^3, \tag{10}$$

where $n(r)$ in units of (m^{-3} cm^{-1}) is a drop-size distribution function specified in the literature for various fog and cloud conditions [7], [15]–[18]. In general, significant values of w (>0.001 g/m^3) require a saturated or slightly supersaturated air mass (100–101 percent RH). Fog described as "light-moderate-heavy" covers values of w in the range "0.001 – 0.05 – 1 g/m^3" (expected maxima in water content are 0.4 for advection and 1 g/m^3 for radiation fog), nonprecipitating clouds contain between 0.1 and 1 g/m^3, and in rain clouds w can exceed 2 g/m^3. Droplets exist well below freezing since water can stay in a supercooled liquid state down to −40°C.

In the atmosphere, substantial variations of w occur in space and time. Lack of data on the particle distribution in the radio path normally precludes quantitative comparisons with propagation predictions. Measurements of mass content w at a point in space or averaged over a radio path are difficult. Direct methods for measuring w consist of extracting a known volume through a cotton pad or of rotating cups in an impeller apparatus, both to be weighed; also, resistance changes can be measured with a hot wire probe attached to an aircraft flying through clouds [17]. When size spectra $n(r)$ are available, an integration according to (10) may be performed. Indirect

techniques determine w from radio-wave responses to suspended particles. Transmission loss or atmospheric emission can be detected at single or multiple frequencies [9], [19]–[21]. Visibility at optical wavelengths also relates to w; however, interdependence between optical attenuation and water content is not unique, but depends strongly on the size distribution $n(r)$ [18].

C. Validity of Rayleigh Model

Refractivity properties of suspended particles were approximated by (5). Only two variables are required, namely permittivity $\epsilon(f, T)$ and mass content w. For (5) to be valid, the radio wavelength (c/f) must be much larger than the particle diameters $(2r)$. Principal modal radii r_0 for SWD size spectra lie between 1 and 20 μm [15]. Consequently, the size distribution $n(r)$ sets an upper frequency limit. To estimate that limit, we compared simultaneous Rayleigh and full-series Mie calculations [7], [19]. The following submillimeter-wave attenuation rates were reported for a distribution $n(r)$ representing the case ($w = 1$ g/m^3, $T = 20$°C, $r_0 = 6$ μm but sizes $r \geq 50$ μm contributing less than 1 percent to w) of a heavy cumulus cloud [7]:

f	α(Mie)	α(Rayleigh)	$\alpha_R/\alpha_M - 1$
(GHz)	(dB/km per g/m^3)		(percent)
300	15.0	15.0	0
400	20.5	20.3	−1
500	26	25	−4
800	41	38	−7
1000	50	43	−14

These results suggest that (5) accounts in a credible manner for propagation effects of SWD up to about 300 GHz when drop sizes are limited to $r \leq 50$ μm. This gravitational size cut-off will be exceeded in clouds with strong internal updrafts (cumulonimbus) or when mixed with rain. Other authors place the Rayleigh limit closer to 100 GHz based on an atypical high value for the principal modal radius ($r_0 \approx 20$ μm) [19]. On the other hand, one can interpret results from (5) up to 1 THz as minimum estimates of propagation effects by SWD and SIC media, and be prepared to perform above 100 GHz full Mie calculations when the size spectrum contains a substantial number of larger (≥ 20 μm) drops.

III. Model Predictions

Attenuation and delay rates were evaluated, whereby $\alpha(f)$ derives from (2), (6c), (8) or (9), (10) and $\tau(f)$ from (4), (3), (6b), (8) or (9), (10). Fig. 1 displays SWD results for frequencies between 0 and 1000 GHz at several temperatures. Selected numerical values of SWD and SIC predictions are listed in Table I. Basically, water permittivity is converted by (6) into droplet refractivity spectra as shown in Fig. 2. Experimental $\epsilon(f, T)$ data were Rayleigh-transformed and demonstrate a much improved fit when compared with single-Debye (SD) predictions. For a least squares fit of 72 selected complex permittivity data ($f = 5 - 1050$ GHz, $T = -4$ to 30°C), the overall rms deviation between experimental and double Debye (DD) model data was $\delta N = 0.011$ (as compared

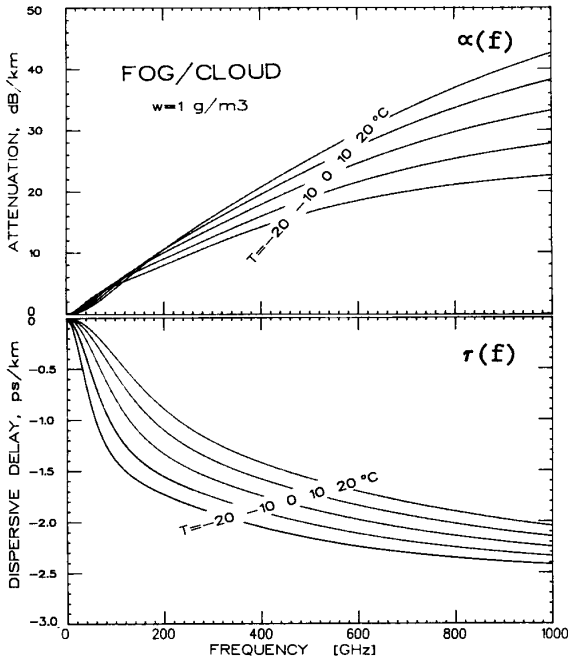

Fig. 1. SWD model predictions of attenuation $\alpha(f)$ and delay $\tau(f)$ for frequencies up to 1000 GHz assuming a water content, $w = 1$ g/m^3, and temperatures from −20 to +20°C (numerical examples are listed in Table I).

to 0.027 for SD). One notices good agreement below 100 GHz; above that frequency, the agreement is only moderate for 10°, 19/20°, and 30°C data (4° and 25°C data were excluded from the fit) [11]. Some 380 data pairs $\epsilon(f, T)$ are available between 0.1 and 100 GHz, but less than ten have been reported (see Fig. 2) between 100 and 200 GHz. New measurements of ϵ are needed above 100 GHz at atmospheric temperatures. Below 300 GHz, attenuation rates for ice crystals are much lower than for water droplets (Table I), and differential phase delay is negligible ($N_i' \approx 0$).

Loss spectra $N''(f)$ display a maximum. Magnitude and frequency position of the maximum follow simple expressions when (8b) is reduced to a single-Debye approximation by setting $\epsilon_2 = \epsilon_1$; that is,

$$N''_{\max}(f_R) = w(9/2)[2(\epsilon_0 + 2)(\epsilon_1 + 2)]^{-1}, \qquad (11a)$$

at the effective relaxation frequency

$$f_R = f_P(\epsilon_0 + 2)/(\epsilon_1 + 2) \qquad (11b)$$

($f_R \approx 170$ to 280 GHz for $T = 0$ to 30°C). Results from (11) are close to DD predictions (see Fig. 2). Dielectric loss $\epsilon''(f)$ of water peaks to a value $(\epsilon_0 - \epsilon_1)/2$ at the principal Debye frequency f_P [≈ 9 to 22 GHz for 0 to 30°C according to (8d)]. Droplets are sparsely distributed in space and their depolarization field leads to much higher relaxation frequencies.

A. Approximation for SWD Attenuation

Over a limited temperature range ($\Delta T \approx \pm 10$°C), the simple approximation

$$\alpha = wa\theta^b \quad \text{dB/km} \qquad (12)$$

TABLE I
SELECTED ATTENUATION AND DELAY RATES BETWEEN 5 AND 1000 GHz
(SWD—water droplets, [SIC]—ice crystals)

	SWD [SIC] Attenuation α/w			SWD Delay τ/w		
T =	-20°C	0°C	20°C	-20°C	0°C	20°C
GHz	dB/km per g/m³			ps/km per g/m³		
5	0.049 [0.00005	0.023 0.00011]	0.013	-0.017	-0.004	-0.001
10	0.190 [0.00021	0.092 0.00037]	0.053	-0.067	-0.016	-0.005
20	0.684 [0.00082	0.360 0.0014]	0.212	-0.241	-0.060	-0.021
30	1.32 [0.0018	0.776 0.0031]	0.470	-0.461	-0.130	-0.045
40	1.97 [0.0033	1.32 0.0056]	0.818	-0.677	-0.217	-0.079
50	2.56 [0.0051	1.91 0.0087]	1.25	-0.866	-0.316	-0.120
70	3.54 [0.0100	3.21 0.0170]	2.29	-1.146	-0.522	-0.218
100	4.66 [0.0205	5.09 0.0347]	4.14	-1.395	-0.800	-0.388
200	7.90 [0.082	9.92 0.139]	10.5	-1.73	-1.34	-0.897
300	11.2 [0.184	14.0 0.312]	15.8	-1.91	-1.58	-1.22
400*	14.2 [0.328	17.8 0.555]	20.6	-2.05	-1.75	-1.42
500	16.6 [0.512	21.4 0.867]	25.2	-2.16	-1.88	-1.58
700	19.9 [1.00	27.3 1.70]	33.3	-2.31	-2.07	-1.81
1000	22.6 [2.05	33.2 3.47]	42.6	-2.42	-2.25	-2.05

* f ≥ 300 GHz: Minimum estimates based on Rayleigh approximation(5)

is sufficient to estimate SWD attenuation rates. Frequency-dependent coefficient $a(f)$ and exponent $b(f)$ were determined from fits of model predictions (Eqs. (2), (6c), (8) to polynomials in power of frequency (GHz) as follows:

$$a(f)=x_0+x_1f+x_2f^2 \quad \text{and} \quad b(f)=y_0+y_1f+y_2f^2, \quad (12a)$$

where x_n and y_n ($n = 0, 1, 2$) are given in Table II, calculated at 10°C and approximately valid for a temperature range of $0°C \le T \le 20°C$. Two frequency ranges each cover x_n ($f = 0 \le 100 \le 1000$ GHz) and y_n ($0 \le 250 \le 1000$ GHz) separately. Exponent $b(f)$ indicates a strong temperature dependence for $\alpha(f)$, changing from 8.3 (10 GHz) to 0 (152 GHz) to -3.8 (1000 GHz).

IV. Millimeter-Wave Study of a Fog Event

Field measurements of atmospheric propagation have been conducted routinely at four millimeter-wave frequencies and at an optical wavelength (0.85 μm) over a short ($L = 0.81$ km) line-of-sight path by the Radio Research Laboratory in a suburb of Tokyo, Japan [14]. A fog observed during the spring of 1985 provides the opportunity to test the frequency dependence predicted by the SWD model outlined in Section II. Attenuation and dispersive delay contributions between 25

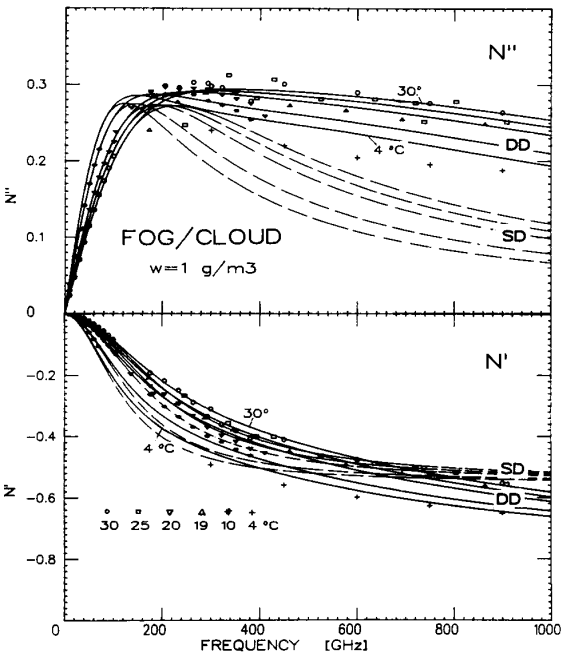

Fig. 2. Complex Rayleigh spectra $N(f)$ of SWD medium. Solid lines: SWD model calculations with double-Debye model DD (8), temperatures decrease from top to bottom as 30, 25, 20, 10, 4°C; dashed lines: same as above, but single-Debye ($\epsilon_2 = \epsilon_1$) model SD for $\epsilon(f, T)$; symbols: experimental ϵ data between 30 and 4°C [11] which were Rayleigh-transformed by (6).

TABLE II
COEFFICIENTS FOR (12) TO ESTIMATE SWD ATTENUATION OVER A TEMPERATURE RANGE 10 ± 10°C

	n = 0	1	2
	a) f = 0 to 100 GHz:		
x =	0.00	$2.18\cdot10^{-3}$	$3.90\cdot10^{-4}$
	b) 100 to 1000 GHz:		
x =	-2.24	$7.02\cdot10^{-2}$	$-2.05\cdot10^{-5}$
	a) f = 0 to 250 GHz:		
y =	9.73	$-8.92\cdot10^{-2}$	$1.73\cdot10^{-4}$
	b) 250 to 1000 GHz:		
y =	-1.12	$-3.04\cdot10^{-3}$	$3.60\cdot10^{-7}$

and 250 GHz, based on MPM predictions [1] for the prevailing meteorological conditions, are exhibited in Fig. 3 and enumerated for the test frequencies in Table III. The test frequencies (f_{1-4} = 50.44, 81.84, 140.66, and 245.52 GHz) were placed in atmospheric window regions remote from spectral lines of the main molecular absorbers oxygen and water vapor.

A. Experimental Arrangement

Line-of-sight propagation measurements were performed over a horizontal path about 20 m above the ground (100 m

TABLE III
MPM PREDICTIONS OF ATTENUATION (α) AND DELAY (τ) FOR AIR PLUS FOG WITH AN SWD CONTENT, w = 0.10 g/m^3
[P = 100 kPa, T = 10°C, RH = 0 (dry) and 100 percent (saturated)]

	f_1=50.44	f_2=81.84		f_3=140.66	f_4=245.52 GHz	
MEDIUM	α_1	α_2	τ_2	α_3	α_4	τ_4
	dB/km	dB/km	ps/km	dB/km	dB/km	ps/km
Dry Air	0.33	0.06	-1.01	0.02	0.02	-0.56
H_2O Vapor	0.16	0.39	0.52	1.25	3.92	5.19
Fog	0.156	0.349	-0.042	0.722	1.264	-0.126

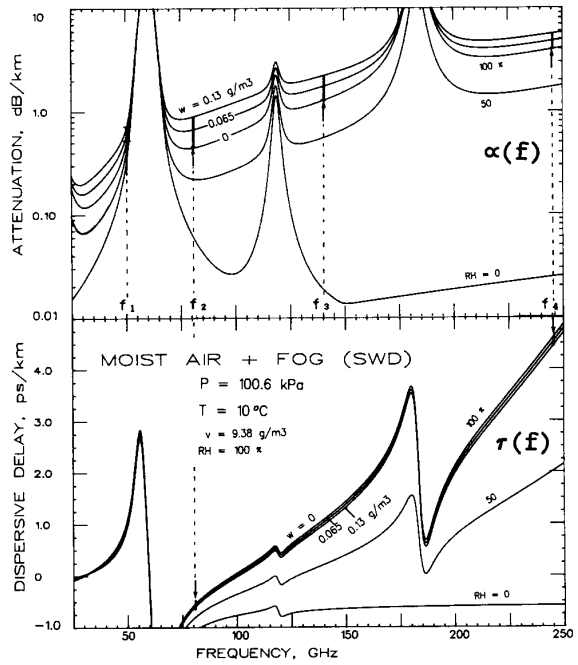

Fig. 3. MPM predictions of moist air propagation effects at sea level conditions (P = 100 kPa; T = 10°C; RH = 0, 50, 100 percent, saturation water vapor concentration, v = 9.38 g/m^3). Fog contributions, w = 0.065 and 0.13 g/m^3, are modeled with the SWD model (Section II) and added to RH = 100 percent.

above sea level) by transmitting horizontally polarized signals. Details of the experimental system have been described elsewhere [14]. Received signal levels A_{1-4} (dB) at f_{1-4} and differential phase changes between f_4 and f_2,

$$\Delta B_{4,2} = B_4(f_4) - 3B_2(f_2) \quad \text{deg}, \tag{13}$$

were recorded digitally by sampling once every minute. It follows from (2) that $\alpha = A/L$ and from (3) that the differential phase change is proportional to the difference in either atmospheric refractivities or propagation delays; i.e.,

$$\Delta\beta = \Delta B/L = 294.9\ [N'(f_4) - N'(f_2)]$$
$$= 88.40\ [\tau(f_4) - \tau(f_2)] \quad \text{deg/km}. \tag{14}$$

The phase measurements are the first ever reported on fog at millimeter-wave frequencies. Stabilities of received signal amplitudes were within ±0.1 dB and of phase differences within ± 1.5 deg for ambient temperature variations between 8° and 12°C. All four links were parallel to each other over a horizontal scale of 4 m. At transmitter and receiver, the antenna diameters were 50 cm for f_2 and 30 cm for the other three frequencies. Temperature T, relative humidity RH, and barometric pressure P were measured at the receiving end by a platinum resistor thermometer, a capacitive thin-film hygrometer, and an aneroid barometer, respectively. Absolute humidity v (g/m^3) was calculated from relative humidity and temperature data [2], [4]. In addition, wind speed and direction were recorded. The average meteorological conditions were assumed to be valid all along the short path.

B. Fog Observations

The fog event chosen for analysis was recorded during early morning of March 18, 1985, from 2:35 to 3:40 JST (Japan Standard Time). Fig. 4(a) depicts the temporal variation of 1-min average values from 1:30 to 4:30 JST for received signal responses. A 7 dB decrease of the signal level from the optical link indicated at 0:40 that haze had formed as precursor to fog. At that time, the rising relative humidity had reached RH = 98 percent, temperature was T = 11.5°C and falling slowly, pressure stayed at P = 100.6 kPa, while the atmosphere was calm (wind speed below 1.5 m/s) and remained so (stagnant moist air was trapped over ground that cooled, conceivably because of radiative heat loss). At 2:35, a sudden decrease below the 30 dB detection threshold of the optical system indicated fog. Temperature was now 10.8°C and continued to decrease to a minimum of 9.5°C (2:50) and then to climb again, typical for a radiation fog undergoing periods of formation and dissipation. Stable millimeter-wave signals were received during the fog period, which lasted until 3:40. At that time the optical signal returned to the "clear air" level while the temperature had reached 11.2°C and wind speed picked up to 3 m/s, removing all fog from the path.

C. Results and Discussion

The millimeter-wave fog responses were isolated (see Fig. 4(b)) by normalizing the received signal levels to baselines A_i

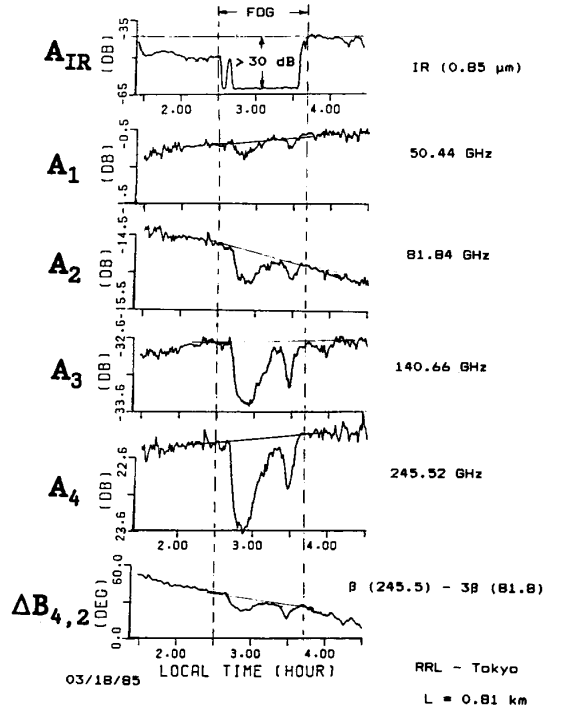

Fig. 4. Time series of recorded path attenuations A_1 (50.4 GHz), A_2 (81.8 GHz), A_3 (140.7 GHz), A_4 (245.5 GHz = $3f_2$), and differential phase delay $\Delta B_{4,2}$ (13). (a) Recorded signal levels including fog. (b) Isolated fog event.

$= 0$ dB and $\Delta B = 0$ deg, defined as a straight line drawn between data levels recorded before the optical signal faded and after it recovered. During the fog, absolute vapor humidity changed only slightly from 10 to 9.5 g/m^3; all but A_2 reflect that trend. The 81.8 GHz receiving antenna lacked a protective hood, and it is suspected that the anomalous baseline slope was caused by dew forming on its PTFE (polytetrafluoroethylene) radome which, in addition, had 2.8 times more effective area than the other three hooded antennas. The fog response of A_2 was not affected. A scatter

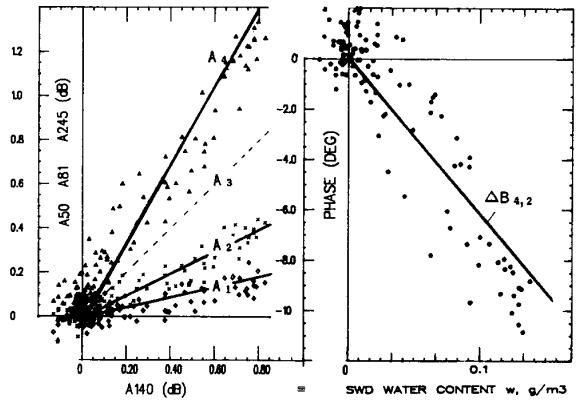

Fig. 5. Scatter plot (1-min averages) of the fog event exhibited in Fig. 4(b). Plotted are attenuations $A_{1,2,4}$ versus A_3 and diff. phase $\Delta B_{4,2}$ versus w. Solid lines: SWD model predictions; symbols: $\diamond$ A_1, $\times$ A_2, $\triangle$ A_4. The highest average experimental SWD concentration is $w = 0.128$ g/m^3.

plot of all 1-min data from Fig. 4(b) demonstrates in Fig. 5 the good correlation to a common variable, selected to be the A_3 signal level.

For a comparison of measurements and predictions, the A_3 level was converted to path-averaged water content following a technique described in [21]. The SWD model (2), (6c), and (8) was implemented to calibrate at f_3 and 10°C (Table III): $A_3 = \alpha_3 L = 0.585$ dB for $w = 0.10$ g/m^3 ($L = 0.81$ km). The two abscissae in Fig. 5 are equivalent. Within experimental uncertainties ($\delta A = \pm 0.1$ dB, $\delta(\Delta B) = \pm 1.5$ deg), the measured data are consistent with model predictions. While experimental errors of the propagation experiment could be assessed, the accuracy relevant to model predictions is not so clear. It relates to uncertainties in the permittivity data for water, discussed in Section III and graphically illustrated in Fig. 2.

V. Conclusion

A spectral characterization of fog/cloud conditions in terms of suspended particle mass content and temperature was given for frequencies that justify the Rayleigh approximation of Mie's scattering theory. That upper frequency limit was placed around 300 GHz with useful estimates extended to 1 THz. Microwave and millimeter-wave attenuation and phase delay effects of atmospherically suspended water droplets and ice crystals were formulated in terms of physical variables to be consistent with the refractivity parameterization of the MPM program [1], [2].

Rates for SWD attenuation and phase delay are based on the double-Debye model (8), which is an up-to-date formulation for the permittivity of liquid water [11]. Compared with single-Debye models, SWD attenuation rates are higher at frequencies above 100 GHz, a fact already suspected in [10]. The results allow more reliable predictions of radio path propagation effects in the 100 to $\geq$300 GHz range and improve retrieval methods for remote sensing applications [19], [20].

A propagation experiment provided data to analyze a fog event. The results tend to confirm SWD predictions between 50 and 246 GHz. Additional experimental fog and cloud

propagation studies are recommended, especially at frequencies above 100 GHz where experimental data are scarce.

Acknowledgment

The authors wish to thank J. P. Stricklen for his skillful programming efforts.

References

[1] H. J. Liebe, "An updated model for millimeter wave propagation in moist air," *Radio Sci.*, vol. 20, no. 5, pp. 1069–1089, Sept.-Oct. 1985.

[2] ——, "MPM—An atmospheric millimeter-wave propagation model," *Int. J. Infrared Millimeter Waves*, vol. 10, no. 6, pp. 631–650, June 1989.

[3] T. Manabe, Y. Furuhama, T. Ihara, S. Saito, H. Tanaka, and A. Ono, "Measurements of attenuation and refractive dispersion due to atmospheric water vapor," *Int. J. Infrared Millimeter Waves*, vol. 6, no. 4, pp. 313–322, Apr. 1985.

[4] T. Manabe, R. O. Debolt, and H. J. Liebe, "Moist-air attenuation at 96 GHz over a 21-km line-of-sight path," *IEEE Trans. Antennas Propagat.*, vol. AP-37, no. 2, pp. 262–266, Feb. 1989.

[5] H. C. Van de Hulst, *Light Scattering by Small Particles*. New York: Wiley, 1957.

[6] C. M. Platt, "Transmission of submillimeter waves through clouds and fogs," *J. Atmos. Sci.*, vol. 27, pp. 421–425, May 1970.

[7] V. J. Falcone, Jr., L. W. Abreu, and E. P. Shettle, "Atmospheric attenuation of millimeter and submillimeter waves: Models and computer code," U.S. Air Force Geophys. Lab., Hanscom Air Force Base, MA, AFGL Tech. Rep. TR-79-0253, Oct. 1979 (AFGL Res. Paper 679).

[8] S. M. Kulpa and E. A. Brown, "Near-millimeter wave technology base study," DARPA Rep. HDL-SR-79-8, U.S. Army MDRC, vol. 1, Nov. 1979.

[9] J. B. Snider, F. O. Guiraud, and D. C. Hogg, "Comparison of cloud liquid content measured by two independent ground-based systems," *J. Appl. Meteor.*, vol. 19, no. 5, pp. 577–580, May 1980.

[10] S. M. Kulpa and E. A. Brown, "Absorption of near-millimeter radiation by liquid fogs," in *Conf. Dig. 4th Int. Conf. Infrared and Millimeter Waves*, Miami Beach, FL, Dec. 10–15, 1979 (IEEE Catalog No.: 79CH138-7 MTT, pp. 30-32).

[11] T. Manabe, H. J. Liebe, and G. A. Hufford, "Complex permittivity of water between 0 and 30 THz," in *Conf. Dig. 12th Int. Conf. Infrared and Millimeter Waves*, Lake Buena Vista, FL, Dec. 14–18, 1987 (IEEE Catalog No.: 87CH2490-1, pp. 229–230). (See also T. Manabe, H. J. Liebe, and G. A. Hufford, "Complex permittivity of water in millimeter, submillimeter, and far-infrared wave regions," Inst. Elec. Commun. Eng., Japan, Yonezawa Conf., Rep. AP 87-121, Feb. 12, 1988.)

[12] G. A. Hufford, "A model for the permittivity of ice from 0 to 1000 GHz," URSI Nat. Radio Sci. Meet., Jan. 4–6, 1989, Boulder, CO, p. 14.

[13] E. E. Altshuler, "A simple expression for estimating attenuation by fog at millimeter wavelengths," *IEEE Trans. Antennas Propagat.*, vol. AP-32, no. 7, pp. 757–758, July 1984. (See also Addendum, *IEEE Trans. Antennas Propagat.*, vol. AP-34, no. 8, p. 1067, Aug. 1986).

[14] Y. Furuhama, T. Manabe, T. Ihara, K. Tohma, K. Kitamura, and Y. Imai, "Experimental study of propagation characteristics in millimeter wave region," in *Proc. URSI Commission F Symp.*, Louvain, Belgium, ESA SP-194, June 1983, pp. 165–171.

[15] D. A. Stewart and O. M. Essenwanger, "A survey of fog and related optical propagation characteristics," *Rev. Geophys. Space Phys.*, vol. 20, no. 3, pp. 441–495, Aug. 1982.

[16] H. E. Gerber, "Relative-humidity parameterization of the navy aerosol model (NAM)," Naval Res. Lab., Washington, DC, NRL Rep. 8956, Dec. 1985.

[17] D. Baumgardner, "An analysis and comparison of five water droplet measuring instruments," *J. Climate Appl. Meteor.*, vol. 22, pp. 891–910, May 1983.

[18] H. E. Gerber, "Liquid water content of fog and haze from visible light scattering," *J. Climate Appl. Meteor.*, vol. 23, pp. 1247–1252, Aug. 1984.

[19] L. Tsang, J. A. Kong, E. Njoku, D. H. Staelin, and J. W. Waters, "Theory for microwave thermal emission from a layer of cloud or rain," *IEEE Trans. Antennas Propagat.*, vol. AP-25, no. 5, pp. 650–657, Sept. 1977.

[20] R. G. Issacs and G. Leblonde, "Millimeter wave moisture sounding: The effect of clouds," *Radio Sci.*, vol. 22, no. 3, pp. 367–377, May-June 1987.

[21] T. S. Chu and D. C. Hogg, "Effects of precipitation on propagation at 0.63, 3.5, and 10.6 microns," *Bell Syst. Tech. J.*, vol. 47, no. 5, pp. 723–759, May-June 1968.

Hans J. Liebe (M'66–SM'72–F'87) was born in Insterburg, Germany, in 1934. He received the Vordiplom (BSEE), Diplom (MSEE) and Doktor-Ingenieur (Ph.D.) degrees, all in electrical engineering, from the Technical University of West Berlin, Germany, in 1957, 1959 and 1964, respectively.

From 1958 to 1964 he was a Research Assistant at the Institute for Microwave Engineering, Technical University Berlin. In 1965 he came to the United States. After a spell with the U.S. Army Signal Corps, Fort Monmouth, NJ, he joined the Quantum Electronics Department of TRG, Melville, NY, where he was involved in investigating new millimeter-wave techniques at 260 GHz. Since 1966 he has been with the Institute for Telecommunication Sciences, NTIA, Department of Commerce, Boulder, CO, where he is now a Senior Research Engineer. He has been working on experimental, analytical, and theoretical aspects of atmospheric propagation characteristics from 1 to 1000 GHz. As recipient of a Humboldt Award he stayed during 1976/1977 at the Max-Planck-Institut for Aeronomy, Lindau and the DFVLR (now DLR), Oberpfaffenhofen, West Germany.

Dr. Liebe has been invited to serve on URSI and IEEE commissions and to contribute to NASA Workshops. He is a member of Commissions A and F of the International Union for Radio Science and of CCIR Study Group 5; he also is a co-investigator of the SPACELAB Mission EOM 3/4-MAS, participates in ITRA (Intercomp. Transmitt. Radiance Algor.) exercises conducted by the International Radiation Commission, and consults on the Electromagnetic Properties of Materials Program of NIST, Boulder, CO.

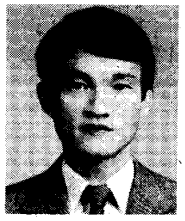

Takeshi Manabe (M'88) was born in Osaka, Japan, on September 19, 1952. He received the B.S., M.S., and D.E. degrees in electronics engineering from Kyoto University, Kyoto, Japan, in 1975, 1977, and 1980, respectively.

In 1980, he joined the Radio Research Laboratory, Ministry of Posts and Telecommunications, Tokyo, Japan. He has been engaged in research on radio wave propagation characteristics at centimeter and millimeter wavelengths in the atmosphere. From 1986 to 1987, he was with the National Telecommunications and Information Administration, Institute for Telecommunication Sciences, Boulder, CO, as a Visiting Scientist. In 1988, he was temporarily transferred to ATR Optical and Radio Communications Research Laboratories, Osaka, Japan.

Dr. Manabe is a member of the Institute of Electronics, Information and Communication Engineers of Japan, and of the Physical Society of Japan.

George A. Hufford (S'45–A'48–M'55) was born in San Francisco, CA, in 1927. He received the B.S. degree in engineering from Cal Tech in 1946, the M.S. degree in electrical engineering from the University of Washington in 1948, and the Ph.D. degree in mathematics from Princeton University, Princeton, NJ, in 1953.

Since 1964 he has been with NTIA and its predecessor organizations. His research has been concerned with radio propagation under real-world conditions as when irregular terrain and a changing atmosphere are involved. He currently is with a group studying the effects of the atmosphere on the propagation of millimeter waves.

Dr. Hufford is a member of the American Mathematical Society, the Society for Industrial and Applied Mathematics, and Sigma Xi.